


2015-01-01

Acoustic Emission Characteristics Of Damage Accumulation In Kevlar® 49 Composites

Eduardo Andrade

University of Texas at El Paso, eddieandrade86@outlook.com

Follow this and additional works at: https://digitalcommons.utep.edu/open_etd

 Part of the [Aerospace Engineering Commons](#), [Materials Science and Engineering Commons](#), and the [Mechanics of Materials Commons](#)

Recommended Citation

Andrade, Eduardo, "Acoustic Emission Characteristics Of Damage Accumulation In Kevlar® 49 Composites" (2015). *Open Access Theses & Dissertations*. 994.

https://digitalcommons.utep.edu/open_etd/994

This is brought to you for free and open access by DigitalCommons@UTEP. It has been accepted for inclusion in Open Access Theses & Dissertations by an authorized administrator of DigitalCommons@UTEP. For more information, please contact lweber@utep.edu.

ACOUSTIC EMISSION CHARACTERISTICS OF DAMAGE
ACCUMULATION IN KEVLAR® 49 COMPOSITES

EDUARDO ANDRADE

Department of Metallurgical and Materials Engineering

APPROVED:

Devesh Misra, Ph.D., Chair

Stephen W. Stafford, Ph.D., P.E.

Pavana Prabhakar, Ph.D.

Charles Ambler, Ph.D.
Dean of the Graduate School

Copyright ©

by

Eduardo Andrade

2015

Dedication

This thesis is in loving dedication to my father and mother whom through words and actions of inspiration and encouragement taught me to pursue my goals and gain high regard of education.

ACOUSTIC EMISSION CHARACTERISTICS OF DAMAGE
ACCUMULATION IN KEVLAR® 49 COMPOSITES

by

EDUARDO ANDRADE, B.S. M.M.E.

THESIS

Presented to the Faculty of the Graduate School of

The University of Texas at El Paso

in Partial Fulfillment

of the Requirements

for the Degree of

MASTER OF SCIENCE

Department of Metallurgical and Materials Engineering

THE UNIVERSITY OF TEXAS AT EL PASO

May 2015

Acknowledgements

I am grateful to Regor Saulsberry and Jess Waller for excellent mentorship and guidance in this work, to Shawn Arnette of TRI (Austin, TX) for supplying K/Ep test specimens, and to Paul Spencer and Ben Gonzalez (WSTF) for assistance with setting up the universal tensile tester. I want to acknowledge the faculty of the Department of Metallurgical and Materials Engineering at UTEP for their insightful knowledge and influence in my educational endeavors.

Abstract

Acoustic emission (AE) data attained during tensile testing of epoxy impregnated Kevlar® 49 (K/Ep) composite strands were reduced and analyzed to monitor progressive damage accumulation during the approach to tensile failure. The K/Ep material tested in this study was chosen due to its similarity to the material-of-construction used in composite overwrapped pressure vessels (COPVs) used on the NASA Space Shuttle Orbiter. Insight into the progressive microstructural degradation of K/Ep strands was gained by monitoring AE event rate and energy. Source location based on energy attenuation and arrival time data was used to differentiate between significant AE attributable to microstructural damage accumulation, and spurious AE attributable to grip and background noise. One of the more notable features observed in the AE data was increasing violation of the Kaiser effect (Felicity ratio < 1.0). The effectiveness of three different stress schedules that allowed the Felicity ratio to be analytically determined is discussed in detail. Potential use of such stress schedules for qualification testing and structural health monitoring of COPV composite materials-of-construction, including carbon-epoxy (C/Ep), is discussed. Future work whereby additional information about progressive damage accumulation is extracted using the modal AE signatures, specifically AE event frequency and velocity information, is also discussed, along with the relevance of anticipated findings.

Table of Contents

Acknowledgements.....	v
Abstract.....	vi
Table of Contents.....	vii
List of Tables	ix
List of Figures.....	x
Chapter 1: Introduction.....	1
Chapter 2: Background	4
Chapter 3: Experimental Apparatus.....	7
3.1 Load Control	7
3.2 Acoustic Emission	9
Chapter 4: Test Conditions	10
4.1 Materials	10
4.2 Load Schedules.....	11
Chapter 5: Results and Discussion	14
5.1 Acoustic Emission Data Reduction	14
5.2 Acoustic Emission Data Interpretation	17

5.3	Felicity Ratio Interpretation.....	21
5.4	Calm Ratio Interpretation	23
Chapter 6: Conclusion		26
References.....		27
Appendix.....		32
Vita		33

List of Tables

Table 1: Distribution of COPVs on Orbiter Space Shuttle.....	4
Table 2: Description of Intermittent Load-Hold Stress Schedules.....	11

List of Figures

Figure 1: Gas and fluid tank locations on the Space Shuttle Orbiter, including helium and nitrogen Kevlar/epoxy (K/Ep) composite overwrapped pressure vessels (COPVs). Photograph and blue arrows: 26-in. diameter Environmental Control and Life Support System nitrogen COPV (six 26-in. nitrogen K/Ep COPVs shown in dark yellow (denoted by number 10); eighteen 19 to 40-in. helium K/Ep COPVs shown in light yellow (denoted by number 6)) [13].	5
Figure 2: AE (left) and tensile test CPU controllers (right).	7
Figure 3: Load control and AE data acquisition system consisting of a electromechanical tensile test instrument.	8
Figure 4: DigitalWave FM-1 8-channel data acquisition system.	9
Figure 5: 4560 denier Kevlar/epoxy tow (25 cm gage length) aligned in grips showing four B1080 AE sensors mounted.	10
Figure 6: Representative intermittent load-hold stress schedule used for Kevlar/epoxy tow characterization (adopted from ASTM E 1067 and E 1118).	12
Figure 7: Representative load-hold stress schedule used for Kevlar/epoxy tow characterization (adopted from NDIS 2421).	13
Figure 8: Typical background noise (channels 1-4): Ch. 1 energy = $0.3588 \text{ V}^2\text{-}\mu\text{sec}$, indeterminate zone location (zone location = -1).	14
Figure 9: Cumulative background AE during an intermittent load hold (ILH method 1) stress schedule test.	15

Figure 10: Representative grip noise (top), and significant AE occurring in the gage region of a Kevlar/epoxy tensile specimen subjected to an intermittent load hold (ILH method 2) stress schedule (bottom)	18
Figure 11: Nonlinear increase in significant AE (red data) during an intermittent load hold (ILH method 2) stress schedule test (blue data)	19
Figure 12: Representative strain (blue data) during an intermittent load hold (ILH method 2) stress schedule test red data).....	20
Figure 13: Dependence of Felicity ratio on stress during an intermittent load hold (ILH method 1) stress	24
schedule test (duplicate results).	24
Figure 14: Dependence of Felicity ratio on stress during an intermittent load hold (ILH method 2) stress schedule test.....	25
Figure 15: Drop in Felicity ratio with increasing load showing least squares fits and 95 % confidence intervals for T1000 carbon-epoxy tow (blue data), IM7 carbon-epoxy tow (green data), Kevlar [®] -epoxy composite tow (red data), and an IM7 composite overwrapped pressure vessel (filled green and black symbols), (NOTE: Felicity ratio determined using the first AE event for Kevlar [®] -epoxy tow, and the mean of the first 15 events for T1000 tow, IM7 tow, and the single IM7 COPV.) [30]	27

Chapter 1: Introduction

For launch vehicles and satellites, the strong drive to reduce weight has pushed Composite Overwrapped Pressure Vessel (COPV) designers to adopt high performance, high specific strength composite materials with a relatively high volume fraction ($v_f \approx 0.6$ to 0.7) of fiber. To date, the composite materials used in COPV designs have typically consisted of aramid or carbon fiber embedded in a thermoset matrix material such as epoxy. The role of the matrix is to transfer pressurization load to the fiber, while the role of the fiber is to withstand the load over time under the environmental exposure conditions encountered in service. Pressurizations of the order of 350 to 700 bar (5,000 to 10,000 psi) are common for COPVs. This has necessitated the use of high load bearing composite overwraps wound around a thin-walled metal liner. Compared to all-metal designs, dual load sharing COPV designs used in NASA Shuttle and International Space Station (ISS) applications represent a dramatic weight savings.

The NDE method-of-choice for detecting and monitoring actively growing flaws and defects is acoustic emission (AE). In this study, AE proved to be an excellent tool for detecting the onset of significant damage in uniaxial K/Ep tow specimens taken to failure. Efforts are underway to look at the modal AE [1] signature, especially the frequency data, to better identify and monitor the underlying mechanisms responsible for damage accumulation. The primary microstructural mechanisms responsible for damage in composite materials such as K/Ep, in order of occurrence are resin cracking, fiber-matrix de-bonding, fiber pullout, and fiber breakage. In COPVs, additional failure mechanisms are operative, such as liner-overwrap separation, liner buckling, and slippage between adjacent tows and overwrap layers. The main advantage gained by testing uniaxial composite tows is easier data reduction since fewer mechanisms are at play. Also, since most of the pressurization load in a COPV designs is

borne by the composite overwrap, it could be argued that the damage progression in individual tows is of preeminent concern and interest.

During the last two decades, many researchers have used AE to study the strain energy release and corresponding stress-wave propagation arising from microstructural changes in composite materials. Early on, researchers recognized that AE is a useful tool for monitoring, in real-time, damage growth in composites [2, 3, 4, 5, 6, 7, 8, 9]. For example, in C/Ep materials matrix cracking is expected to occur at frequencies less than 200 kHz, debonding and pull-out between 200 and 300 kHz, and fiber breakage at greater than 300 kHz [4]. The difficulty in distinguishing between AE events of similar frequency, namely, matrix cracking and fiber/matrix debonding, and the use AE parameters such as signal duration to permit correlation of AE signal with failure mode, have also been described [7, 8]. It is hoped that a more thorough analysis of the modal AE data sets acquired in this study will allow resin cracking, fiber-matrix debonding, fiber pullout, and fiber breakage to be easily distinguished. This, in turn, would allow the precursor damage events to be identified and monitored, since these smaller scale precursor events are what drive damage accumulation at larger length scales until some critical damage state is reached that causes macroscopic failure. In the context of precursor initiation, evolution of accumulated damage, and critical thresholds, AE data has the potential of being able to predict rupture of the composite overwrap in COPV applications.

One of the established tenets describing AE of composites states that if a composite material is loaded, unloaded, and then reloaded, new AE activity will not occur until the highest load previously experienced by the material is exceeded. This phenomenon is known as the Kaiser effect, and is observed in materials that behave elastically during reloading, i.e., have undergone negligible plastic or permanent deformation (viscous loss processes) during previous loadings. However, once damage begins to accumulate in fiber reinforced polymer (FRP) structures, the Kaiser effect begins to be

violated and new AE activity will occur in subsequent loadings (or COPV pressurizations) before the highest previous load (or pressure) is reached. The analytical parameter that describes departure from the Kaiser effect is known as Felicity ratio (FR) given by:

$$\text{FR} = \text{stress level where AE begins in load cycle} / \text{maximum previous stress}$$

When $\text{FR} = 1.0$, the Kaiser effect is said to be followed, while for $\text{FR} < 1.0$, the Kaiser effect is said to be violated. Also, the larger the departure of the Felicity ratio at a value less than unity, the more pronounced the accumulated damage. Damage accumulation trends as revealed by FR data have been well documented in AE studies on reinforced concrete composites [10], and are a centerpiece of ASTM standards used for AE qualification of FRP materials [11, 12].

This paper is a reproduction of research conducted at NASA-White Sands Test Facility [13] and focuses on the development of a quantitative AE procedure specific to K/Ep, which has also proven utility for monitoring damage accumulation in C/Ep. It was hoped that the procedures described in this paper would lay the groundwork for establishing critical thresholds for accumulated damage in composite structures such as COPVs so that precautionary or preemptive engineering steps can be implemented to minimize or obviate the risk of catastrophic failure of those structures. This paper details some important advances made towards developing such a procedure.

Chapter 2: Background

NASA has been faced with recertification and life extension issues for K/Ep COPVs distributed throughout various systems on the Space Shuttle Orbiter. There are 24 spherical K/E COPVs on each Orbiter (Figure 1), which can be categorized as follows (Table 1):

Table 1: Distribution of COPVs on Orbiter Space Shuttle

Quantity	Diameter (in)	Description
6	26	Environmental Control and Life Support System (ECLSS) nitrogen COPVs
2	19	Forward Reaction Control Subsystem (FRCS) helium COPVs
4	19	Aft Reaction Control Subsystem (ARCS) helium COPVs
2	40	OMS helium COPVs
7	26	Main Propulsion System (MPS) helium COPVs
3	40	Main Propulsion System (MPS) helium COPVs

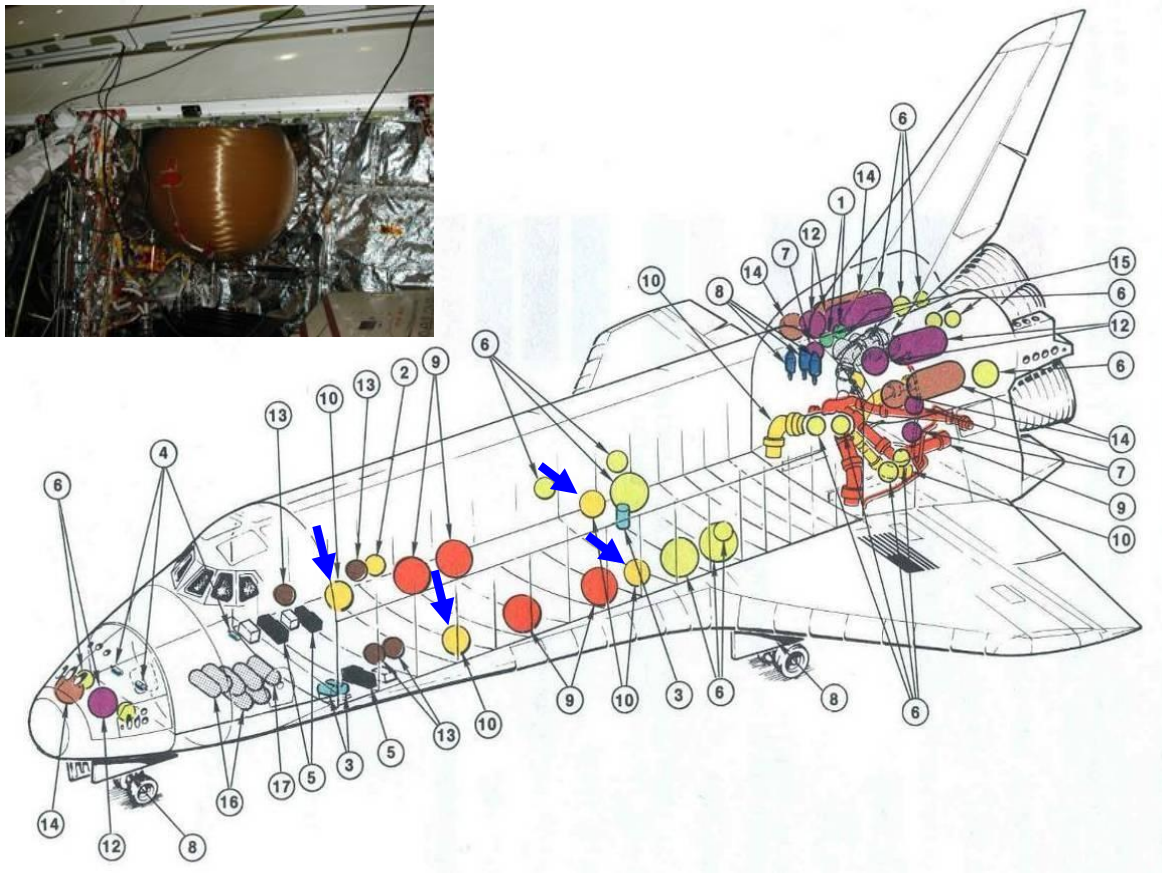


Figure 1: Gas and fluid tank locations on the Space Shuttle Orbiter, including helium and nitrogen Kevlar/epoxy (K/Ep) composite overwrapped pressure vessels (COPVs). Photograph and blue arrows: 26-in. diameter Environmental Control and Life Support System nitrogen COPV (six 26-in. nitrogen K/Ep COPVs shown in dark yellow (denoted by number 10); eighteen 19 to 40-in. helium K/Ep COPVs shown in light yellow (denoted by number 6)) [13].

The Shuttle K/Ep COPVs were designed and developed in the late 1970s and most of the COPVs have been in service since delivery in the 1980s. Each of the Shuttle K/Ep COPVs have varying criticality, usage histories, damage and repair histories, time at pressure, and number of pressure cycles.

The original certification for Shuttle K/E COPVs was for 10 years, which was later extended to 20 years. Shuttle K/E COPVs operating without certification were flown on waiver.

Shuttle K/Ep COPVs are of particular concern due to the insidious and catastrophic “burst-before-leak” (BBL) failure mode caused by stress rupture (SR) of the composite overwrap. SR is a function of composite fiber stress ratio (operating fiber stress divided by fiber strength determined from a burst test for the specific type of COPV under consideration) and time at pressure (typically hundreds or thousands of hours). This failure mode has none of the features of predictability associated with metal pressure vessels, such as predictability of crack geometry, growth rate and size, features that lend themselves to the use of nondestructive evaluation (NDE) methods, for example. In essence, the variability or “surprise factor” associated with SR in K/Ep COPVs cannot be eliminated, and thus, the overwrap and liner combination must be designed so that the SR failure mode is extremely unlikely over the lifetime of the vessel. SR life has been defined by the American Institute for Aeronautics and Astronautics (AIAA) Aerospace Pressure Vessels Standards Working Group as “the minimum time during which the composite maintains structural integrity considering the combined effects of stress level(s), time at stress level(s), and associated environment” [14].

In addition to BBL failure of K/Ep, carbon-epoxy (C/Ep) overwraps are also prone to SR, and are especially sensitive to impact damage. Unfortunately, K/Ep COPV assets used on the Shuttle and C/Ep COPV assets used on the ISS are also not amenable to destructive tests to ascertain the reduction in service life due to stress degradation, or lowering of burst strength due to impact. For these reasons, NASA has devoted much effort to develop nondestructive evaluation (NDE) methods that can be used during in-service inspections and structural health monitoring.

Chapter 3: Experimental Apparatus

3.1 Load Control

Programmed tensile stress schedules were applied to 4560 denier (nominal) K/Ep tow specimens using an Instron[®] 5569 Series Electromechanical Test Instrument equipped with a 50 kN (11,200 lbf) capacity load cell (Figure 3). Other features included self-tightening 25 × 50 mm (1 × 2 in.) wedge action mechanical grips, and a Windows compatible Bluehill[®] (version 1.8.289) (Figure 2, right). To minimize excessive AE during loading and unloading ramps, a 20 N/min (4.5 lbf/min) loading/unloading rate was used, consistent with the ASTM E 1118 [12] recommendation that the load rate should not exceed 5 percent per minute of the desired highest stress (in this case, the UTS). To prevent saturation of the Bluehill[®] data acquisition buffer, a 1 to 2 sec⁻¹ data acquisition rate was used, depending on the duration of test (tests generally took 7 to 16 h to complete). Real-time stress and strain data were recorded during all tests. Tensile test data acquired was synchronized with AE data acquired to facilitate monitoring of progressive damage accumulation as a function of applied stress.



Figure 2: AE (left) and tensile test (right) system CPU controllers.

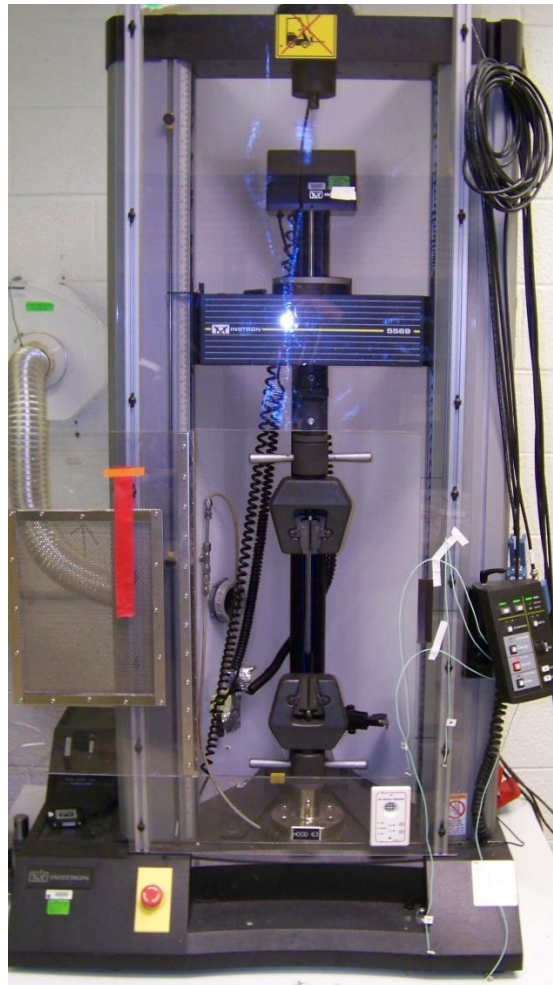


Figure 3: Load control system: Instron[®] 5569 Series Electromechanical Tensile Test Instrument.

3.2 Acoustic Emission

AE measurements were taken using a DWC FM-1 (DigitalWave Corp., Centennial, CO) system equipped with 8-channel capability, four of which were used in this study (Figure 4). Each channel was connected to a DWC PA-0, 0 dB Gain preamplifier, and then to a broadband, high fidelity B1080 piezoelectric sensor with a frequency range 1 kHz to 1.5 MHz (output signals were noisy and nonlinear at the lower 1 to 200 kHz end of the claimed frequency response range). The AE system was supported with a lunchbox computer equipped with WaveExplorer™ software (version 6.2.0) (Figure 2, left). The software allowed arrival time, event energy, and event time to be acquired for all registered events. Sensor sensitivity was checked using pencil lead breaks performed midway between adjacent sensors (midpoint of sensors 1-2, 2-3, and 3-4), according to guidelines described in ASTM E 976 [15]. The FM-1 setup parameters were as follows: Preamp: 5 (gain x 6 dB), signal: 24 (gain dB), signal: 20 (HP filter (kHz)), trigger: 3 (gain x 3 dB), trigger: 20 (gain dB), trigger: 50 (HP filter kHz), trigger (LP filter MHz) (Figure 4).



Figure 4: AE DigitalWave FM-1 8-channel data acquisition system.

Chapter 4: Test Conditions

4.1 Materials

Unidirectional 4560 denier Kevlar® 49 composite strands (ca. 1987, received from Texas Research Institute, Austin, TX) had an ultimate tensile strength (UTS) of 1312 ± 67 N (295 ± 15 lbf) and an ultimate percent elongation (ϵ^*) of 3.1 ± 0.2 percent. The density of the Kevlar® was 144 kg/m^3 . Each tensile specimen was prepared per ASTM D 2343 [16] and had elliptical cross-sectional areas of 0.347 mm^2 (0.000544 in^2), with a nominal thickness of 1.1 mm (0.043 in.), a width of 1.4 mm (0.055 in.), and a gage length of 25 cm (10 in.). Each specimen had cardboard end tabs with dimensions: $1 \times w = 5 \times 2.5 \text{ cm}$ ($2 \times 1 \text{ in.}$). Tow ends were secured to the cardboard with a bead of adhesive (type unknown). The specimens were mounted vertically with sensors positioned approximately 5 cm (2 in.) from each other and the cardboard tabs (Figure 5). Sensors were mounted using Lord 202 adhesive with accelerator 17 (Lord Corp, Cary, NC) mixed at a ratio of approximately ten parts adhesive to one part accelerator.

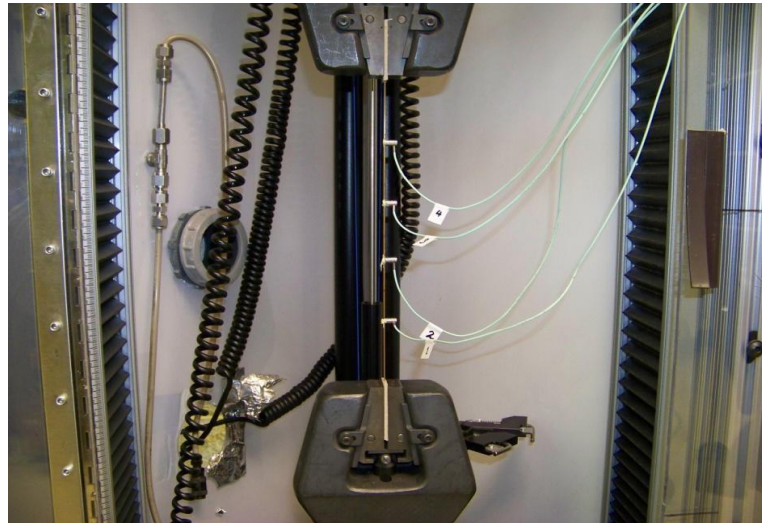


Figure 5: 4560 denier Kevlar/epoxy tow (25 cm gage length) aligned in grips showing four B1080 AE sensors mounted.

4.2 Load Schedules

Three different stress schedules were used. The first two schedules were based on the pressure tank examination procedure described in ASTM E 1067 [11], similarly referred to as the manufacturer's qualification test in ASTM E 1118 [12]. The load sequence began with an initial hold period between 10 and 30 min to determine the level of spurious AE attributable to background noise as the specimen was held in an unloaded state. These two procedures will be described generically as intermittent load-hold (ILH) stress schedules in this paper, and more specifically as ILH1 and ILH2 (Table 2). The ILH1 method encompassed stresses between 530 N (120 lbf) and rupture, and allowed the onset of the first significant AE to be determined. The ILH2 method was developed to impose more load-holds between rupture and the region where significant AE was first observed (around 890 N (200 lbf)). Therefore, it was hoped the ILH2 method would yield more information about the damage evolution closer to rupture. In retrospect, the 60:30 N (2:1) loading:unloading ratio used in the ILH2 method was inadequate (ILH2 Steps 3 and 5, Table 2), and a ratio closer to 50:20 N (2.5:1) probably would have more suitable (ILH1 Steps 3 and 5, Table 2). The ILH1 stress schedule is method is shown in Figure 6, while the ILH2 method is shown in Figure 11.

Table 2: Description of Intermittent Load-Hold Stress Schedules

ILH1	ILH2
1. Ramp: Load to 530 N (120 lb _f)	1. Ramp: Load to 890 N (200 lb _f)
2. 10-min load hold	2. 10-min load hold
3. Ramp: Unload 90 N (20 lb _f)	3. Ramp: Unload 30 N (7 lb _f)
4. 10-min hold	4. 10-min hold
5. Ramp 220 N (50 lb _f) to next highest load	5. Ramp 60 N (14 lb _f) to next highest load
6. Repeat Steps 2-5 until UTS is reached	6. Repeat Steps 2-5 until UTS is reached

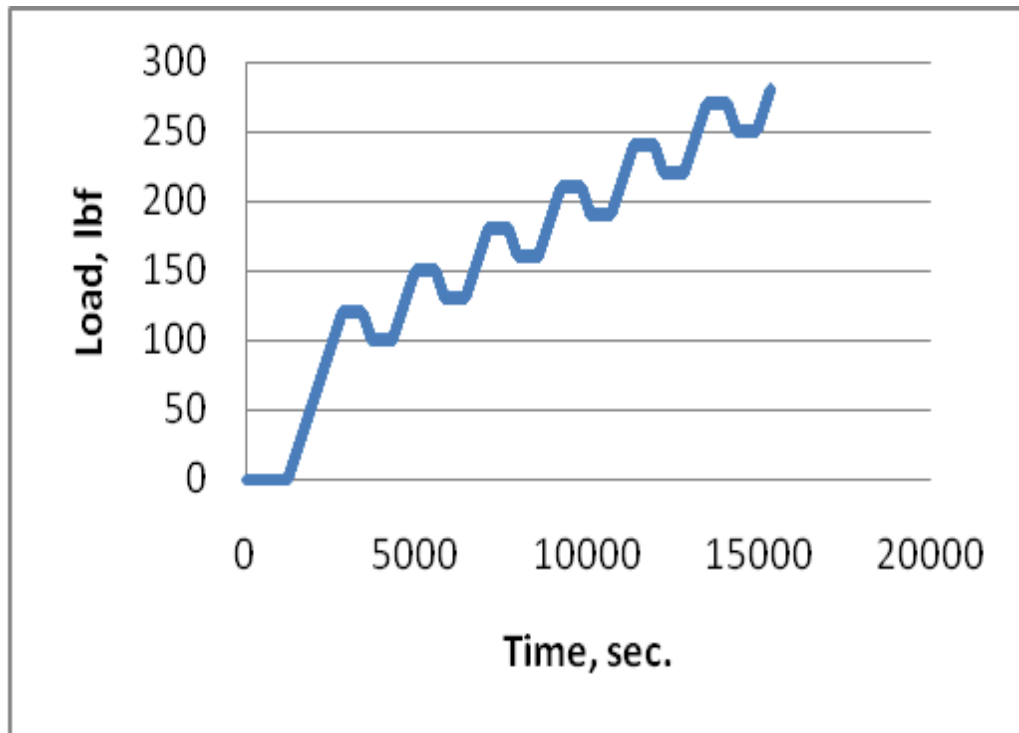


Figure 6: Representative intermittent load-hold stress schedule used for Kevlar/epoxy tow characterization (adopted from ASTM E 1067 and E 1118)

The Japanese Society for Non-Destructive Inspection (JSNDI) developed an alternate stress schedule that has been successfully used to characterize reinforced concrete failure [17]. Like the ILH1 and ILH2 methods, the Japanese practice detects violations of the Kaiser effect through measurement of the FR, but proposes another index value for assessing accumulated damage; namely, the Calm Ratio (CR). Unlike the FR, the CR is attributable to the occurrence of significant AE during unloading cycles, but like situations where the $FR < 1.0$, is also indicative of accumulated damage. Analytically, the CR is determined using the expression:

CR = accumulated AE events during the unloading portion of a stress schedule / accumulated events during the preceding loading cycle

The Japanese practice has been successfully used by Lovejoy [10] to assess the severity of damage in concrete. In this method, denoted ILH3, the FR and CR are plotted against stress, and the intersection point of the linear least squares fits determined, to give the critical CR threshold below which incipient or intermediate damage occurs and above which intermediate or severe damage occurs. Application of the ILH3 stress schedule (Figure 7) to K/Ep gave an opportunity to test the validity of JSNDI approach (Standard unavailable) to a fiber reinforced composite material.

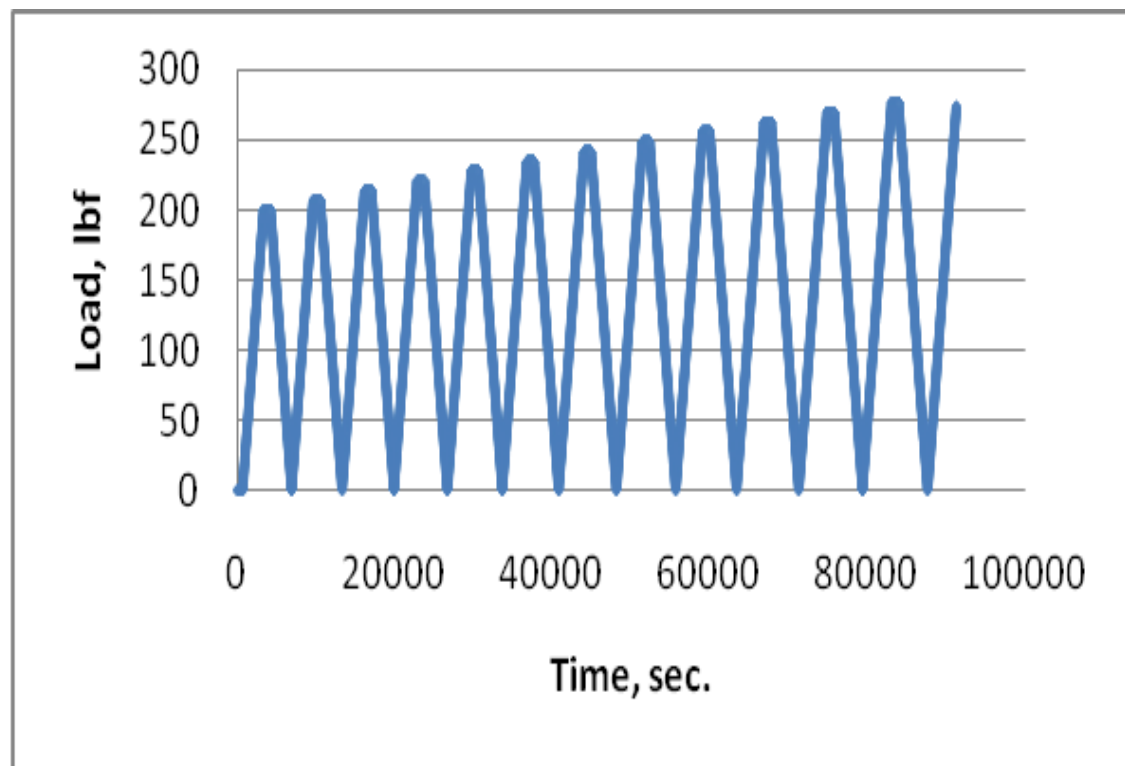


Figure 7: Representative load-hold stress schedule used for Kevlar/epoxy tow characterization (adopted from NDIS 2421)

Chapter 5: Results and Discussion

5.1 Acoustic Emission Data Reduction

Background noise checks were performed before each programmed stress schedule to determine the level of spurious AE. Typical characteristics of spurious AE (Figure 8) were: 1) low energy (< 0.5 $V^2\text{-}\mu\text{sec}$), and 2) indeterminate source location as revealed by 0, 1 or 2 arrival times. Such events were categorized by the WaveExplorer™ software as having a nonsensical zone location = -1.

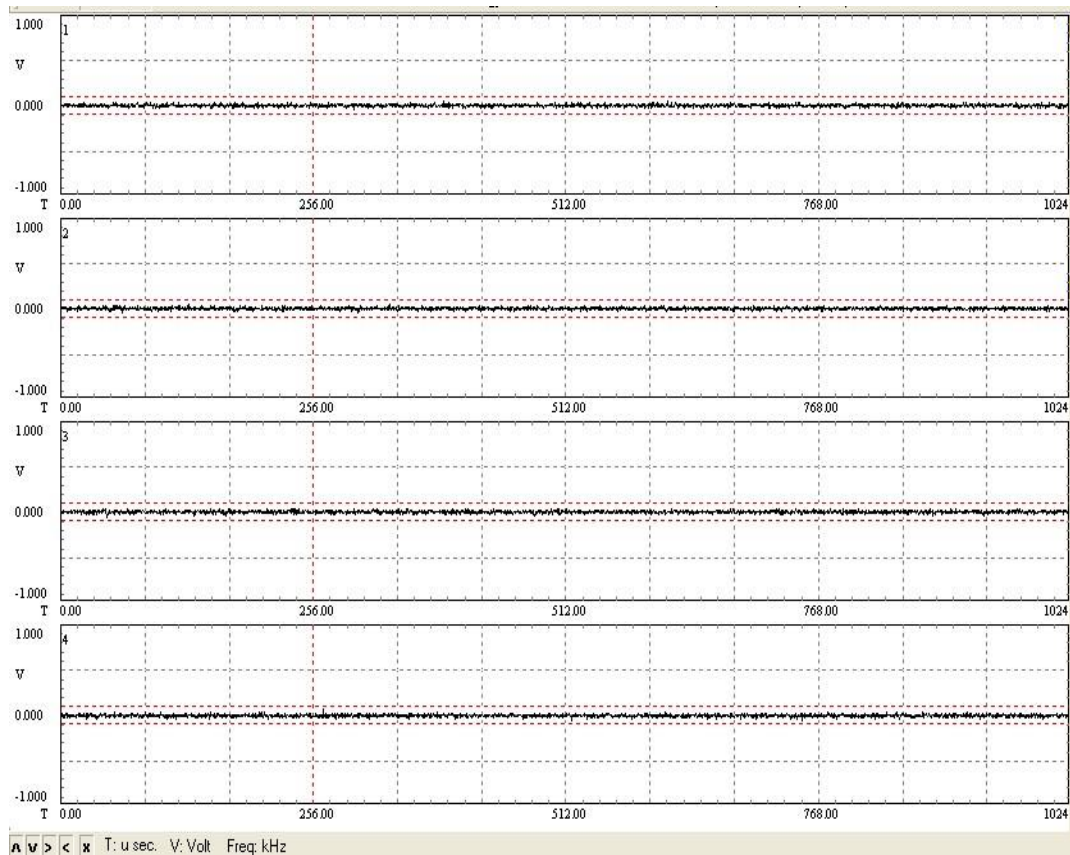


Figure 8: Typical background noise (channels 1-4): Ch. 1 energy = $0.3588 V^2\text{-}\mu\text{sec}$, indeterminate zone location (zone location = -1)

Further verification that AE events such as the one depicted in Figure 8 were actual background noise was obtained by showing that the background AE event rate did not change with respect to the applied stress schedule (Figure 9). Further analysis of the AE background data revealed a nearly constant background count rate equal to about 1.8 counts/min during successive (Step 5, Table 2) ILH1 plateaus of increasing applied stress, offering further verification that the AE events such as the one depicted in Figure 8 were spurious.

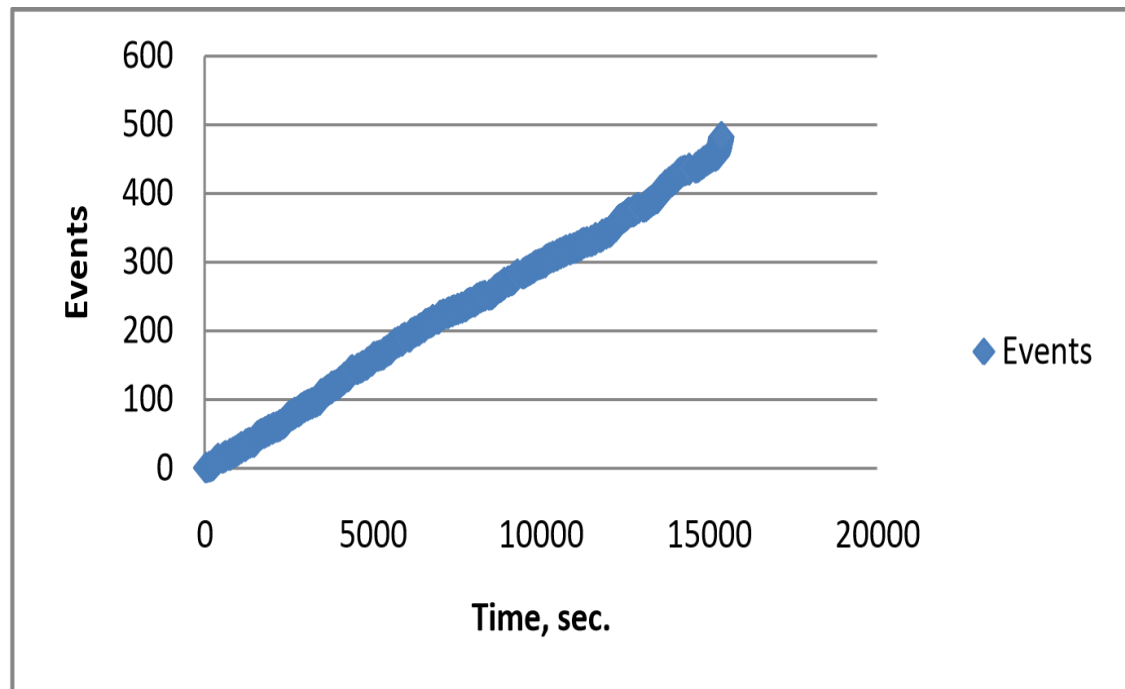


Figure 9: Cumulative background AE during an intermittent load hold (ILH method 1) stress schedule test.

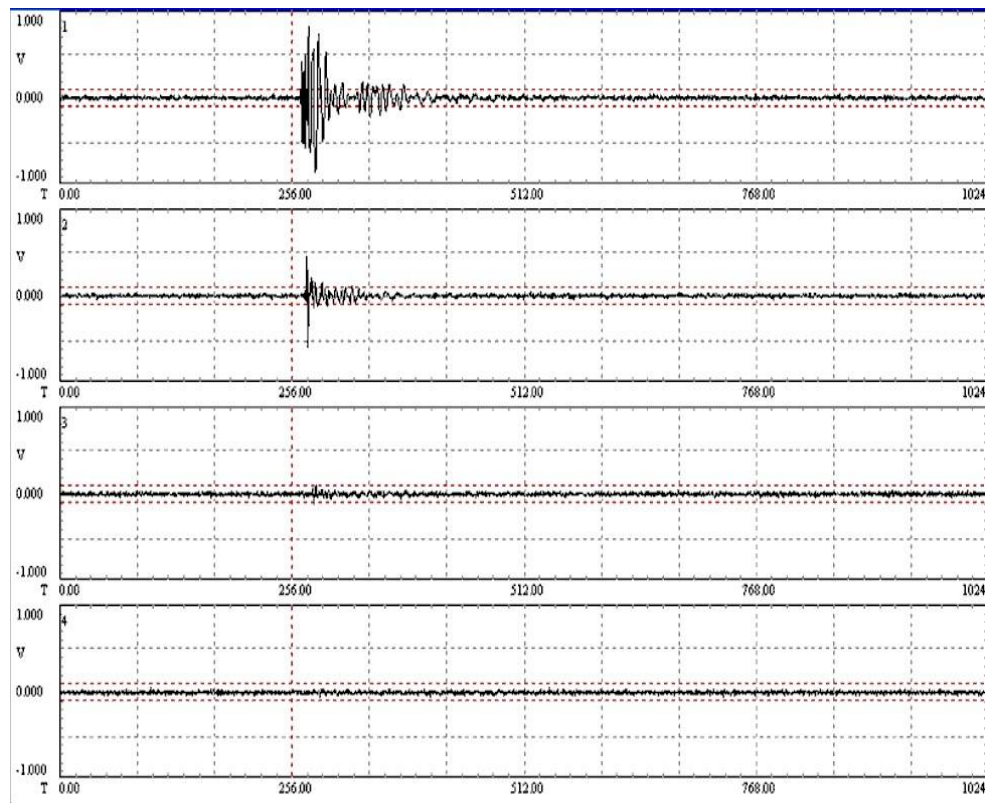
Once spurious AE was removed from the AE data sets, AE events indicative of probable grip noise were identified. Typical characteristics of grip noise were: 1) low energy ($< 0.7 \text{ V}^2\text{-}\mu\text{sec}$), and 2) first arrival times at either sensor 1 or 4 as revealed by trending arrival time data at two or more sensors (for example, $t_1 < t_2 (< t_3 < t_4)$) for grip noise originating in the grip closest to sensor 1, or conversely, $t_1 > t_2 (> t_3 > t_4)$) for grip noise originating in the grip closest to sensor 4. AE events detected only at

sensor 1 or 4 (only t_1 or t_4 existed), and meeting the above $< 0.7 \text{ V}^2\text{-}\mu\text{sec}$ energy requirement, were also categorized as grip noise. Qualitatively, the AE signature of grip noise was indistinguishable from that of spurious background noise, and had the same appearance as the AE signature shown in Fig. 8. At the time this paper was written, a more thorough arrival time, energy, and frequency analysis was underway to further differentiate between valid low energy grip noise, and low energy events that may have been attributable instead to matrix cracking, de-bonding, and pull-out, that happened to occur closest to sensors 1 and 4.

Additional details of the data filtering process were as follows. The $0.5 \text{ V}^2\text{-}\mu\text{sec}$ low energy threshold, quoted above for spurious background AE, was calculated by averaging all the energies measured at the first arrival channel. AE events with energies that exceeded this threshold were examined using source location. All events that were determined to originate outside gage length were removed from the data set (grip noise, Figure 8, top), while all events that were determined to originate within the gage length were retained (gage events of interest, Figure 8, bottom). Events that did not register source location data (only 1 or 2 arrival times observed) were then analyzed using energy distribution. First, each channel's energy was compared to the $0.5 \text{ V}^2\text{-}\mu\text{sec}$ threshold. Each channel 1-4 had to exceed a fixed threshold equal to 25 percent of the average energy above the average energy of the channel. Events that did not exceed the threshold were removed from the data set. Due to the proximity of sensors 1 and 4 to the grips, channels 2 and 3 were then analyzed according to their energies. These channels had to exceed a fixed threshold equal to 25 percent of the maximum energy for spurious background AE above the average energy at each specified channel. The events that exceeded this threshold were then combined with the source locatable events and were then renumbered relative to time.

5.2 Acoustic Emission Data Interpretation

Significant, source-locatable AE that exceeded the above energy threshold screening criterion, and also the originated in the gage region of the specimen (Figure 10, bottom) was found to occur at loads above 890 N (200 lbf), which in turn corresponds to an elapsed time of 11,000 sec. in the ILH2 method (Figure. 11). Another feature observed was a dramatic increase in the AE count rate as failure was approached, or analogously, the cumulative number of AE events as shown in Figure 11. Nonlinear increases in the AE event rate are described in ASTM E 1067 and E 1118 as corresponding to regions of critically intense AE activity indicative of accumulated, severe damage. Also of note is the fact that these regions also show the greatest violation of the Kaiser effect, and therefore, the lowest FR values. Similarly, the highest CRs should be observed in such regions.



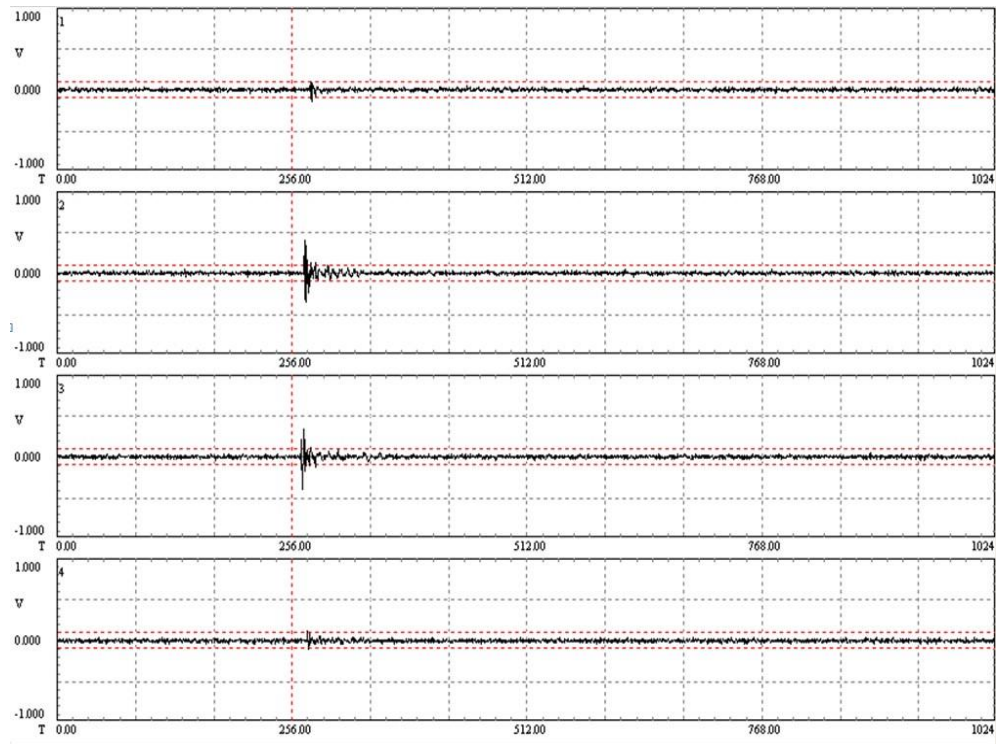


Figure 10: Representative grip noise (top), and significant AE occurring in the gage region of a Kevlar/epoxy tensile specimen subjected to an intermittent load hold (ILH method 2) stress schedule (bottom)

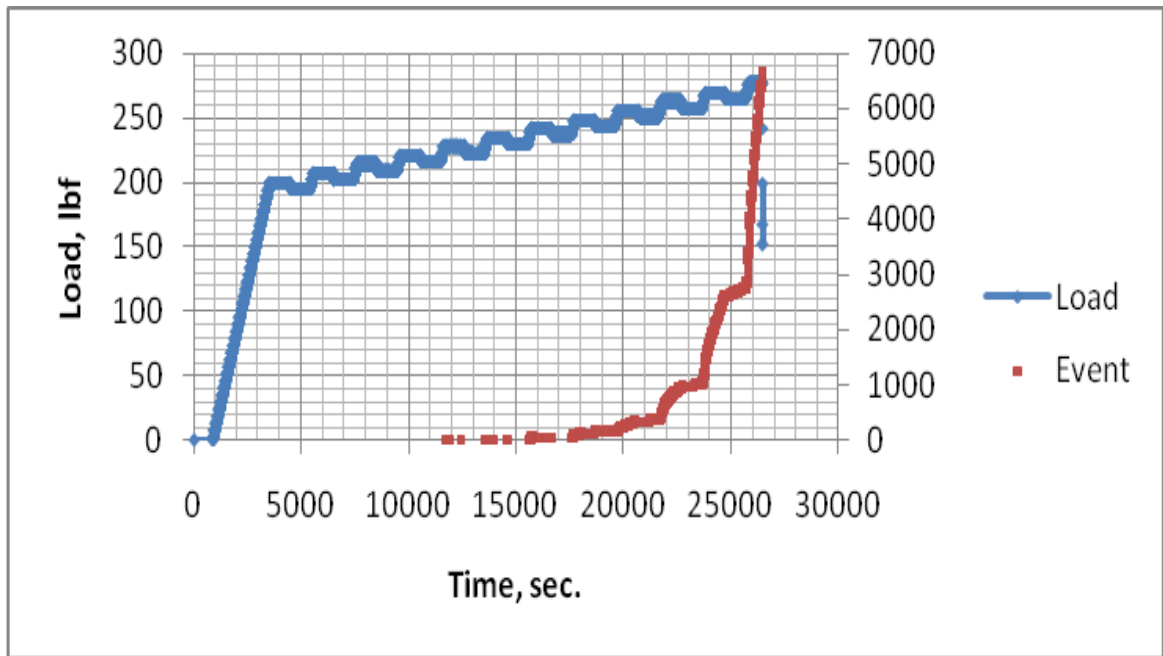


Figure 11: Nonlinear increase in significant AE (red data) during an intermittent load hold (ILH method 2) stress schedule test (blue data)

The strain data is also known to correlate with acoustic emission data and give a fair indication of the proximity of failure. In fact, studies have shown that the strain rate in creep tests reaches a minimum about 2/3rds the way to failure in specimens held at constant stress [18]. Other investigators have shown that outbursts of AE activity often coincide with discontinuous changes in strain [19]. However, for purposes of this investigation, it was sufficient to show that the ultimate strain was in agreement with published values. For example, an ultimate strain data of about 3.5 percent was observed at conclusion of the ILH2 stress schedule test (Figure 12), which compared favorably to the value of $\epsilon^* = 3.1 \pm 0.2$ percent reported for the K/Ep tested in the study.

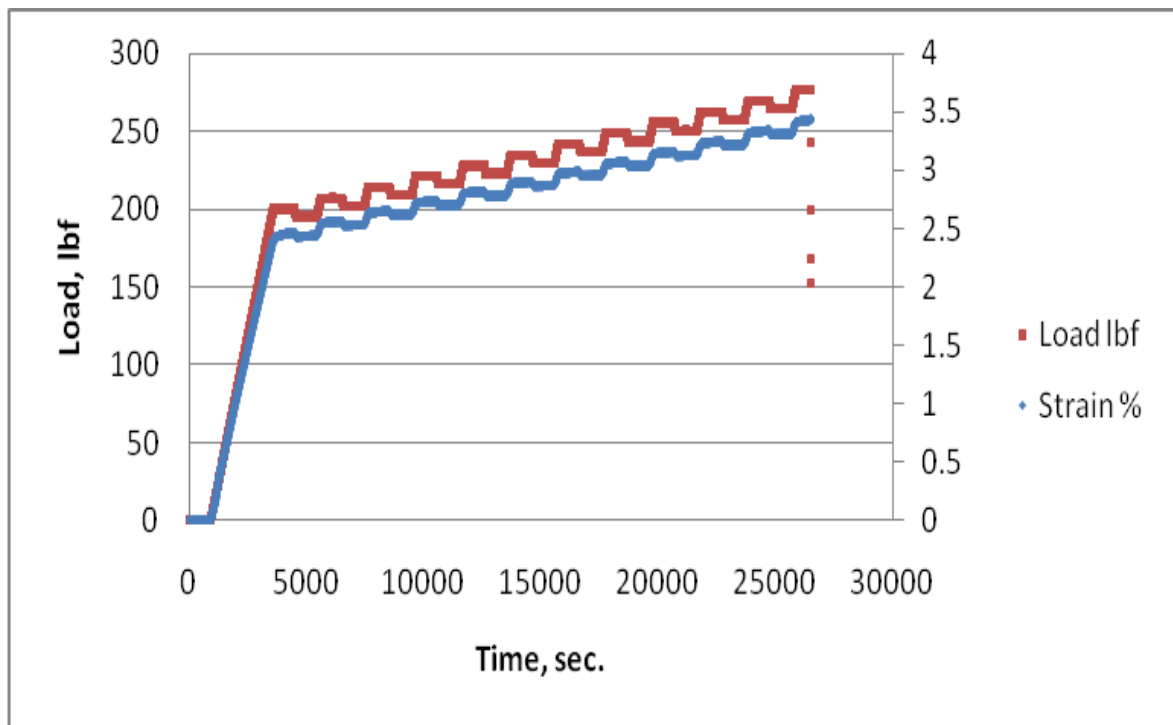


Figure 12: Representative strain (blue data) during an intermittent load hold (ILH method 2) stress schedule test (red data).

5.3 Felicity Ratio Interpretation

The most significant finding of the present investigation was the linear decrease in the FR with increasing stress during the ILH1 method (Figure 13, duplicate data), and the ILH2 method (Figure 14). As was mentioned earlier, the 60:30 N (2:1) loading:unloading ratio used in the ILH2 method was inadequate (ILH2 Steps 3 and 5, Table 2), since sequential holds when the specimen was unloaded were equal to the penultimate highest stress, instead of being higher than the penultimate highest stress, which is the accepted ASTM practice. Therefore, adopting a loading:unloading ratio closer to 50:20 N (2.5:1) probably would have been more suitable (ILH1 Steps 3 and 5, Table 2), possibly leading to better results and a higher correlation coefficient than the 0.866 value observed. Still, the correlation coefficients observed indicated good ($R^2 = 0.866$) to excellent ($R^2 = 0.985$) agreement.

The duplicate agreement obtained in the ILH1 method is also instructive. Taking $FR = 1$ as the threshold for significant accumulated damage, stress thresholds of 1054 N (237 lbf) were obtained in both cases. The ILH2 method, despite its poorer correlation coefficient, predicted an onset of significant damage in the vicinity of 1070 N (240 lbf). This remarkable agreement suggests that COPV materials-of-construction, namely, K/Ep and C/Ep tows, and COPVs themselves, could be qualified using ILH-type stress schedules, to make sure no accumulated damage has occurred. Also, since stress and time are nearly equivalent from a physical aging standpoint, accelerated test methodologies could be developed whereby the stepped elevated stress schedules could be used to predict the threshold of significant damage occurring at lower stress, i.e., operational COPV pressures, subjected to creep loading for prolonged periods of time.

Examination of AE energies also gave a similar indication of accumulated damage (data not shown). At the $FR = 1.0$ threshold, quite energetic events in excess of $10 \text{ V}^2\text{-}\mu\text{sec}$ began to be observed. It is presently unknown if such events are indicative of fiber rupture. Efforts are presently underway to

look at the frequency of these high energy events, since fiber rupture is expected to occur above 300 to 400 kHz. The broadband sensors used in this study should be ideally suited for picking up damage signatures in this frequency range.

5.4 Calm Ratio Interpretation

CRs were not observed during the IHL2, or strangely enough, during the ILH3 stress schedules. In other words, no significant AE was observed in 2 out of the 3 stress schedules used. However, in the IHL1 case (data not shown), there was enough AE activity during unloading portions of the test to obtain a measurable CR, so that a linear least squares fit to the data could be made, and the intersection point of the linear least squares CR and FR fits determined, to give the critical CR threshold below which incipient or intermediate damage occurred and above which intermediate or severe damage occurred. Development of optimized stress schedules may allow greater exploitation of CR data, and allow quantitative thresholds to for incipient, moderate, and severe damage to be determined for composite materials such as K/Ep and C/Ep.

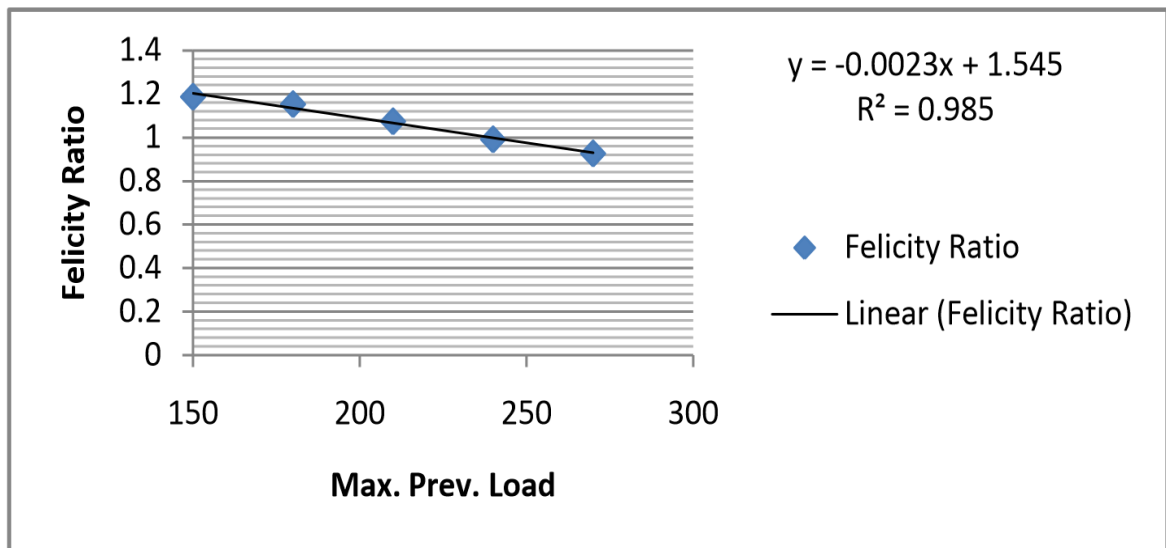
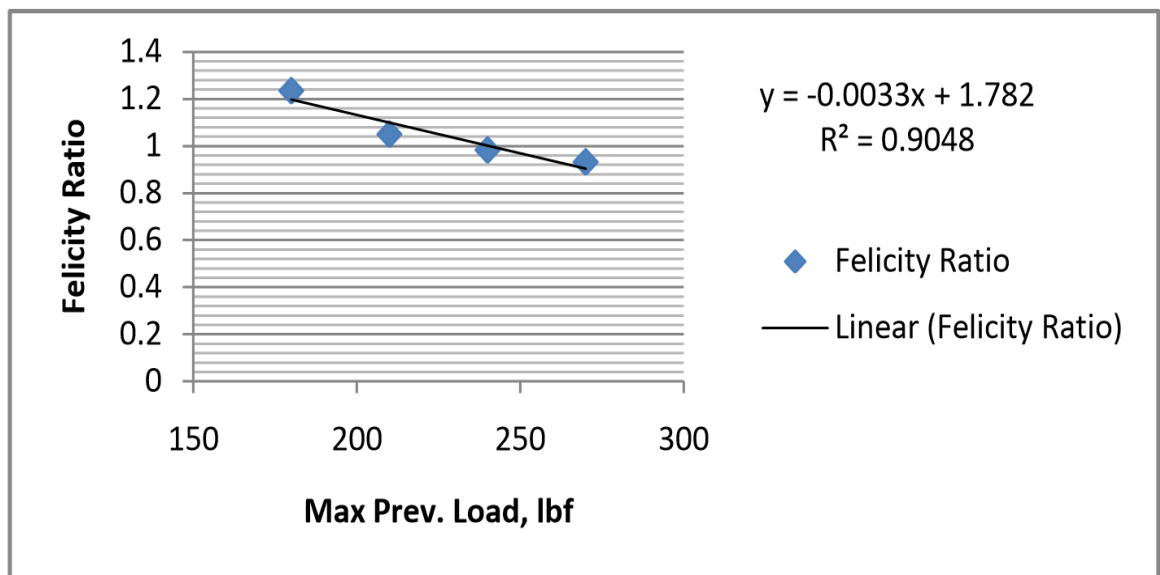


Figure 13: Dependence of Felicity ratio on stress during an intermittent load hold (ILH method 1) stress schedule test (duplicate results).

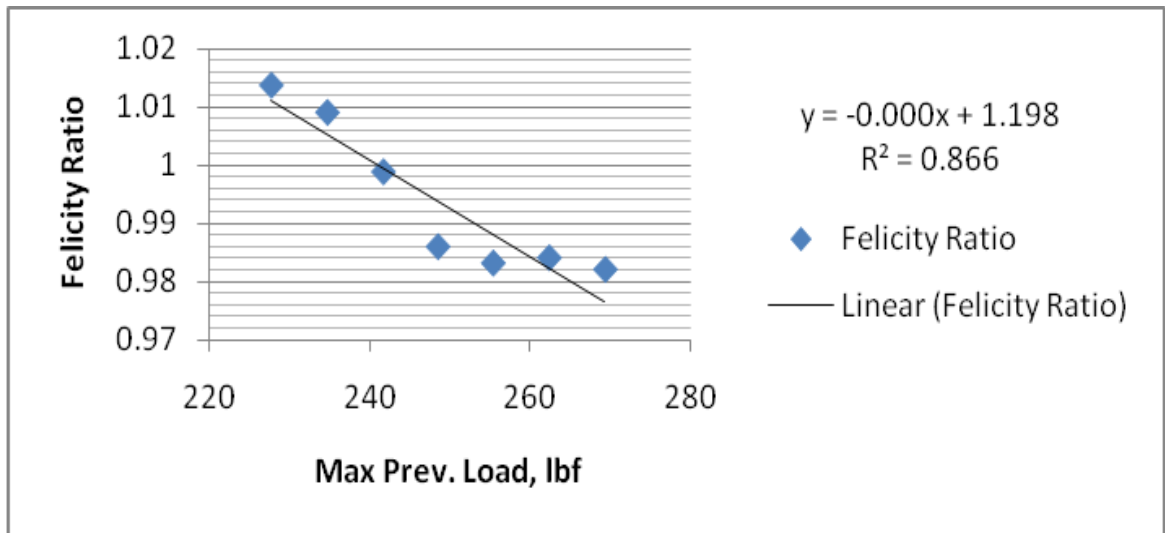


Figure 14: Dependence of Felicity ratio on stress during an intermittent load hold (ILH method 2) stress schedule test

Chapter 6: Conclusion

The most significant contribution in this work was the finding that the Felicity ratio gives a reproducible linear estimate of the stress where significant accumulated damage occurs, which was subsequently presented at the 2009 Quantitative Nondestructive Evaluation (QNDE) Conference [20]. A new parameter referred to as the critical Felicity ratio (FR^*) was later developed in order to implement Felicity ratio calculations on C/Ep [21] alongside the mean method of the first, n , events which were presented at the 2010 (QNDE) Conference [22]. Further automation tools have been developed for calculating Felicity ratio for composites [23] and a conference presentation was given to the 2010 ASNT Conference and Quality Testing Show [24]. Two NASA-JSC Biennial Research and Technology Development Reports were published in 2011 as well [25, 26]. Further numerical and statistical work has been accomplished and presented to enhance the Felicity ratio prediction calculations on composite tows and COPVs [27, 28, 29].

The work in this paper laid the groundwork in K/Ep and has evolved to substantiate meaningful results in C/Ep tow and COPVs shown in (Figure 15). C/Ep tow gave an FR^* observed scatter between 1 and 2 percent while the ultimate tensile strength of C/Ep exhibited more scatter, varying between 5 and 8 percent, indicating that the FR is more independent of failure mode than the tensile strength [30].

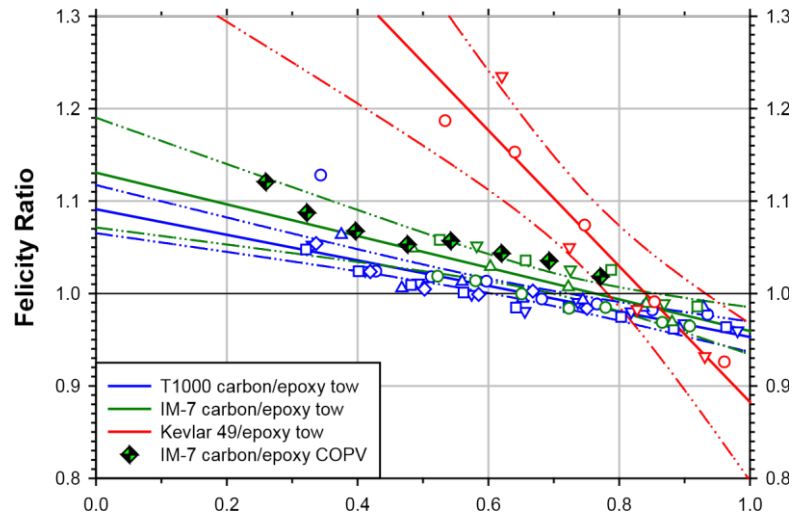


Figure 15: Drop in Felicity ratio with increasing load showing least squares fits and 95 % confidence intervals for T1000 carbon-epoxy tow (blue data), IM7 carbon-epoxy tow (green data), Kevlar[®]-epoxy composite tow (red data), and an IM7 composite overwrapped pressure vessel (filled green and black symbols), (NOTE: Felicity ratio determined using the first AE event for Kevlar[®]-epoxy tow, and the mean of the first 15 events for T1000 tow, IM7 tow, and the single IM7 COPV.) [30]

References

- [1] Gorman, M. R., "Modal AE: A New Understanding of Acoustic Emission," DigialWave Corp., Denver, CO, unpublished work.
- [2] Awerbuch, J., Ghafari, S., "Monitoring Progression of Matrix Splitting During Fatigue Loading Through Acoustic Emission in Notched Unidirectional Graphite/Epoxy Composites," *J. Reinforced Plastics and Composites*, Vol. 7, (1988), 245-263.
- [3] Ely, T., Hill, E., "Longitudinal Splitting and Fiber Breakage Characterization in Graphite Epoxy Using Acoustic Emission Data," *Matl. Eval*, (1995), 288-294.
- [4] De Groot, P., Wijnen, P., Janssen, R., "Real-time frequency determination of acoustic emission for different fracture mechanisms in carbon/epoxy composites," *Composites Sci. Technol.*, Vol. 55, (1995), 405-421.
- [5] Prosser, W. H., Jackson, K. E., Kellas, S., Smith, B. T., McKeon, J., Friedman, A., "Advanced, Waveform Based Acoustic Emission Detection of Matrix Cracking in Composites," *Matls. Eval.*, Vol. 53, No. 9, (1995), 1052-1058.
- [6] Shiwa, M., Carpenter, S., Kishi, T., "Analysis of Acoustic Emission Signals Generated during the Fatigue Testing of GFRP," *J. Composite Matls.*, Vol. 30, No. 18, (1996), 2019-2041.
- [7] El Guerjouma, Baboux, J.-C., Ducret, D., Godin, N., Guy, P., Huguet, S., Jayet, Y., Monnier, T., "Non-Destructive Evaluation of Damage and Failure of Fibre Reinforced Polymer Composites Using Ultrasonic Waves and Acoustic Emission," *Adv. Eng. Matl.*, Vol. 3, No. 8, (2001), 601-608.
- [8] Huguet, S., Godin, N., Gaertner, R., Salmon, L., Villard, D., "Use of acoustic emission to identify damage modes in glass fibre reinforced polyester," *Composites Sci Technol.*, Vol. 62, (2002), 1433-1444.

- [9] Dzenzis, Y. A., Qian, J., “Analysis of microdamage evolution histories in composites,” *Int. J. Solids and Structures*, Vol. 38, (2001), 1831-1854.
- [10] Lovejoy, S., “A General Overview of Acoustic Emission Testing and it’s Applications to Highway Infrastructure,” Oregon Department of Transportation
- [11] ASTM, Practice for Acoustic Emission Examination of Fiberglass Reinforced Plastic Resin (FRP) Tanks/Vessels, E 1067, *American Society for Testing and Materials*, West Conshohocken, PA, 19428-2959, 2001.
- [12] ASTM, Practice for Acoustic Emission Examination of Reinforced Thermosetting Resin Pipe (RTRP), E 1118, *American Society for Testing and Materials*, West Conshohocken, PA, 19428-2959, 2000.
- [13] Andrade, Eduardo, Jess M. Waller, and Regor L. Saulsberry. "Use of Acoustic Emission to Monitor Progressive Damage Accumulation in Kevlar® 49 Composites.", *USRP Technical Report*, NASA-JSC Whites Sands Test Facility, Las Cruces, NM, 2009.
- [14] AIAA S-081A-2006, Space Systems – Composite Overwrapped Pressure Vessels (COPVs), Approved July 24, 2006, American Institute of Aeronautics and Astronautics, 1801 Alexander Bell Drive, Reston, VA 20191.
- [15] ASTM, Guide for Determining the Reproducibility of Acoustic Emission Sensor Response, E 976, *American Society for Testing and Materials*, West Conshohocken, PA, 19428-2959, 2000.
- [16] ASTM, Test Method for Tensile Properties of Glass Fiber Strands, Yarns, and Rovings Used in Reinforced Plastics. D 2343-03. *American Society for Testing and Materials*, West Conshohocken, Pennsylvania, 2003b.
- [17] JSNDI, “Recommended Practice for In Situ Monitoring of Concrete Structures by Acoustic Emission,” NDIS 2421, Japanese Society for Non-Destructive Inspection, 2000.

- [18] Sornette, D., “Statistical Physics of Rupture in Heterogeneous Media,” *J. Mech. Phys. Solids*, (2005): (<http://arXiv.org/abs/condmat/0409524>).
- [19] Waller, J., Saulsberry, R., NASA NDE Working Group website, <http://nnwg.org/current/>, under White Sands Test Facility, “In-Situ NDE Characterization of Kevlar and Carbon Composite Micromechanics for Improved COPV Health Monitoring”, 2008.
- [20] Waller, J., Saulsberry, R. Andrade, E., Use Of Acoustic Emission to Monitor Progressive Damage Accumulation in Kevlar® 49 Composites, *36th Annual Review of Progress in Quantitative Nondestructive Evaluation (QNDE) Conference*, Kingston, RI, July 26-31, 2009.
- [21] Nichols, C. T., J. M. Waller, and R. L. Saulsberry, Acoustic Emission Lifetime Estimation for Carbon Fiber/Epoxy Composite Overwrapped Pressure Vessels, *USRP Technical Report*, NASA-JSC Whites Sands Test Facility, Las Cruces, NM, August 2010.
- [22] Waller, J., Saulsberry, R., Nichols, C., Wentzel, D., Use of Modal Acoustic Emission to Monitor Damage Progression in Carbon Fiber/Epoxy Tows and Implications for Composite Structures, *37th Annual Review of Progress in Quantitative Nondestructive Evaluation (QNDE) Conference*, San Diego CA, July 18-25, 2010.
- [23] Weathers, D. E., C. T. Nichols, J. M. Waller, R. L. Saulsberry, “Automated Determination of Felicity Ratio for Composite Overwrapped Pressure Vessels”, *USRP Technical Report*, NASA-JSC Whites Sands Test Facility, Las Cruces, NM, August 2010.
- [24] Waller, J., .R. Saulsberry, C. Nichols, D. Wentzel, E. Andrade, D. Weathers, E. Kowalski, Use of Modal Acoustic Emission to Monitor Micromechanical Damage Progression in Carbon Fiber/Epoxy Tows and Implications for Related Composite Structures, *ASNT Fall Conference and Quality Testing Show*, Houston, TX, November 18, 2010.

- [25] Waller, J., Nichols, C., Saulsberry, R., Acoustic Emission and Development of Accept-Reject Criteria for Assessing Progressive Damage in Composite Materials, *Biennial Research and Technology Development Report* – Johnson Space Center, December 2011.
- [26] Nichols, C., Waller, J., Saulsberry, R., Johnson, K., Weathers, D., Tylka, J., Intern, Optimized Software Approaches to Predict Rupture in Fracture-Critical Composite Components and Implications for Structural Health Monitoring, *Biennial Research and Technology Development Report* – Johnson Space Center, December 2011.
- [27] Tylka, Jonathan M., Jess M. Waller, Kenneth L. Johnson, and R. L. Saulsberry. "Use of Numerical Analysis of Acoustic Emission Data to Optimize Failure Prediction in Carbon-Epoxy Materials of Construction." *USRP Technical Report*, NASA-JSC Whites Sands Test Facility, Las Cruces, NM.
- [28] Abraham, Arick Reed A., Kenneth L. Johnson, Charles T. Nichols, Regor L. Saulsberry, and Jess M. Waller. "Use of statistical analysis of acoustic emission data on carbon-epoxy COPV materials-of-construction for enhanced felicity ratio onset determination." *USRP Technical Report*, NASA-JSC Whites Sands Test Facility, Las Cruces, NM, 2012.
- [29] Abraham, A. R., E. Andrade, K. L. Johnson, C. T. Nichols, R. L. Saulsberry, J. M. Tylka, J. M. Waller, and D. J. Wentzel. "Developing Novel Acoustic Emission Procedures for Failure Prediction of Carbon-Epoxy COPVs and Related Composite Materials." *Technical Presentation*, NASA-JSC Whites Sands Test Facility, Las Cruces, NM, 2012.
- [30] Waller, Jess, and Regor Saulsberry. "In-Situ Nondestructive Evaluation of Kevlar (Registered Trademark) and Carbon Fiber Reinforced Composite Micromechanics for Improved Composite Overwrapped Pressure Vessel Health Monitoring." *Technical Report*, NASA-JSC Whites Sands Test Facility, Las Cruces, NM, 2012.

Appendix

Subject	RE: Permission for Master's Thesis
From	Saulsberry, Regor L. (WSTF-RF111)
To	Andrade, Eduardo
Sent	Tuesday, April 14, 2015 9:23 PM

Sure, if it has been previously reviewed for a conference paper or otherwise cleared (which I think most of it was). If there is any question we can always run it through for public release.

Thanks,
Regor Saulsberry, P.E.
Project Manager
NASA Materials and Components Laboratories Office
White Sands Test Facility
12600 NASA Road
Las Cruces, NM 88012
Office (575) 524-5518
Mobile (575) 635-7970
Fax (575) 524-5260

Secretary: Elizabeth Nietubyc (575) 524-5723

From: Andrade, Eduardo [<mailto:eandrade2@miners.utep.edu>]
Sent: Tuesday, April 14, 2015 2:35 PM
To: Saulsberry, Regor L. (WSTF-RF111)
Subject: Permission for Master's Thesis

Hello Mr. Saulsberry,

I am wrapping up my thesis for my master's degree in order to graduate this semester and want to ask you for permission to reproduce the work I contributed on USE OF ACOUSTIC EMISSION TO MONITOR PROGRESSIVE DAMAGE ACCUMULATION IN KEVLAR 49® COMPOSITES? The name of my thesis will be Acoustic Emission Characteristics of Damage Accumulation in Kevlar 49® Composites and will be focused on the contributions I made for this publication.

Thank You,
Eduardo Andrade

Vita

Eduardo Andrade was born in El Paso, Texas in the summer of 1986. The second son of Fernando and Maria Andrade, he graduated from Clint High School in Clint, Texas and entered the Metallurgical and Materials Engineering program at the University of Texas at El Paso. While in pursuit of a bachelor's degree, he worked as a student intern for NASA Johnson Space Center at White Sands Test Facility in Las Cruces, NM. Shortly after, he supported continued research activities with NASA through UTEP. After completing the bachelor's degree requirements from the University of Texas at El Paso in May 2011 he worked an engineering summer internship at Alcoa Howmet in Wichita Falls, Texas. He entered the Graduate School at the University of Texas at El Paso in the Fall of 2011 during which he co-founded and developed a renewable energy company, Pasolus, LLC, in El Paso, TX. After gaining entrepreneurial experience he worked as an Applications Engineer for Alcoa Oil and Gas in the Woodlands, TX. At the time of this publication, Eduardo works as a Materials and Process Engineer intern for Boeing in El Paso, TX.

Permanent address: 12636 Wolf Berry Dr.
El Paso, Texas, 79928

This thesis was typed by Eduardo Andrade.